Efficient measurement of broadband terahertz optical activity

Daniel J. Aschaffenburg,[1] Michael R. C. Williams,[1] Diyar Talbayev,[1,a)] Daniel F. Santavicca,[2] Daniel E. Prober,[2] and Charles A. Schmuttenmaer[1,b)]
[1]*Department of Chemistry, Yale University, P.O. Box 208107, 225 Prospect St., New Haven, Connecticut 06520-8107, USA*
[2]*Department of Applied Physics, Yale University, New Haven, Connecticut 06511, USA*

(Received 19 April 2012; accepted 26 May 2012; published online 15 June 2012)

We report a method to determine the four Stokes parameters of each spectral component in a broadband terahertz (THz) pulse by using a continuously rotating analyzer and a standard THz time domain spectroscopy (THz-TDS) instrument. A complete characterization of the polarization state at each frequency is obtained through a single time-domain measurement. Our method requires no specialized THz emitters or detectors; it is, therefore, perfectly general and suitable for any existing THz-TDS apparatus. © *2012 American Institute of Physics*. [http://dx.doi.org/10.1063/1.4729148]

Terahertz (THz) spectroscopy has become a powerful tool for far-infrared studies since its emergence in the late 1980s and early 1990s.[1–3] The study of metamaterials[4,5] and their optical activity at THz frequencies is a rapidly expanding area.[6–11] The optical activity of a sub-wavelength metal helix,[6] random collections of helices,[8] and chiral gammadion lithographic structures[9] has been measured with broadband, linearly polarized THz pulses. Kubarev *et al.* studied a 2D array of metal-semiconductor microhelices using a free electron laser and found a strong resonance at wavelengths of twice the helix length.[10] The linearly polarized light was rotated up to 16.5° at these resonant frequencies. Tzuang *et al.* examined a thin metal film perforated with an array of Archimedean spiral slots and determined the polarization of the resulting THz pulse at two resonances for both left and right-handed spirals that had an average ellipticity of 12.6°.[11]

The optical activity of chiral molecules in the visible and UV regions of the spectrum has been characterized by circular dichroism (CD) and optical rotatory dispersion (ORD) since the early 1800s.[12] Vibrational circular dichroism (VCD) measurements have been carried out in the IR since 1975.[13] To date, no such studies have been performed over a broad spectral range in the THz spectral region due to the high sensitivity required since the optical activity of molecules scales quadratically with frequency.[14] However, using a free electron laser, Xu *et al.*[15] determined the CD of a lysozyme solution at 3 specific frequencies (1.53, 1.98, and 2.52 THz), finding positive CD values for the latter two frequencies and zero CD at 1.53 THz. Improvements of the techniques that will allow the optical activity of similar systems to be measured with tabletop THz spectrometers are naturally of significant interest.

We report here a rapid and highly efficient method for determining the frequency-dependent optical activity (comprising both circular dichroism and optical rotation) of a given sample. A single measurement allows us to determine all four Stokes parameters for each frequency component within the experimental bandwidth. This method does not require specialized THz emitters or detectors, which is an advantage over experiments that use multi-contact photoconductive antennas to simultaneously detect two orthogonal THz polarizations.[16–18] We also show that our method is superior to time-domain THz methods that rely on the measurement of the THz field at two[19,20] or three[21] judiciously chosen analyzer angles, as well as frequency domain methods that make use of incoherent far-infrared light sources and intensity detectors, such as bolometers or Golay cells.[22,23] In our experiment, the only required input is linearly polarized light. This obviates the need for dedicated sources of left-handed circularly polarized and right-handed circularly polarized light (LHCP and RHCP, respectively), which is a significant advantage over incoherent frequency-domain polarimetry. Preparation and analysis of such circularly polarized states in frequency-domain measurements require wave plates and compensators that can be difficult to fabricate and align. More importantly, experiments using these elements become impractical when covering a broad frequency range.

Figure 1 is a schematic diagram of the experiment, which is based on the THz spectrometer described in Ref. 24. A 50 fs mode-locked Ti:Sapphire laser (KM Labs Griffin) with a repetition rate of 80 MHz and center wavelength of 800 nm is used to excite a photoconductive array antenna grown on LT-GaAs (Batop Optoelectronics iPCA 21-05-1000-800-h). The emitter antenna is modulated with a 30 kHz square wave DC bias voltage (± 5 V) to allow detection using a lock-in amplifier (Stanford Research Systems SRS 830). A 50/50 beam splitter is used to direct half the optical power to the THz emitter, and the remaining power to detect the THz pulse on a second, identical LT-GaAs array antenna. The emitter and detector are both polarization sensitive and are oriented in such a fashion as to produce and detect vertically polarized THz radiation. A free-standing wire grid polarizer (13 μm wire diameter, 25 μm spacing) is used to "clean up" the polarization from the emitter. The THz beam path is purged with dry nitrogen to reduce absorption by atmospheric water vapor. Data are collected in the

a)Current address: Department of Physics, Tulane University, New Orleans, Louisiana 70118, USA.
b)Email: charles.schmuttenmaer@yale.edu.

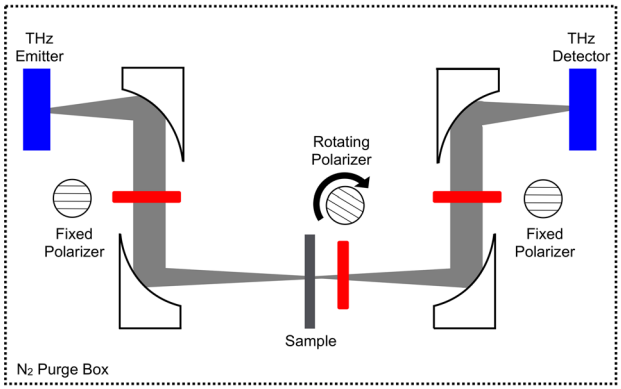

FIG. 1. The experimental schematic for a general THz-TDS setup using the polarimetry method as described in the text. Four off-axis paraboloid mirrors guide and focus the THz pulse from the emitter, through the sample (gray), and then to the detector. Polarizer positions are indicated in red with an adjacent circle that illustrates their orientation if viewed along the beam path. The first fixed polarizer is used to clean up the vertically polarized THz pulse. The rotating polarizer and the second fixed polarizer are placed after the sample and are used to measure its optical activity. The THz setup is purged with N_2, and additional details of the setup are described in the text.

time domain by varying the delay between the THz generation and detection pulses.

Polarimetric capabilities are added to the spectrometer through the use of two additional polarizers placed between the sample location and the detector. The polarizer nearest the detector (free-standing wire grid, 13 μm wire diameter, 25 μm spacing) is fixed at the orientation for optimal transmission of vertically polarized light. The other polarizer (1200 grooves/mm of aluminum on a HDPE substrate) is either rotated in discrete steps using a motorized rotation stage (accuracy of $\pm 0.1^\circ$) or spun continuously (15 Hz) using a modified optical chopper wheel. In the continuously spinning configuration, the lock-in amplifier is referenced to the second harmonic of the frequency at which the polarizer is spun, and a DC bias is used for the THz emitter instead of the 30 kHz square wave. It is possible to substantially improve the signal to noise ratio (SNR) by using a double modulation scheme and two lock-in amplifiers. In this case, the THz emitter uses the original 30 kHz square wave bias, and the signal from the THz detector is sent to a lock-in amplifier using 30 kHz as a reference frequency. The output of the first lock-in is fed to another that uses a reference frequency of twice the polarizer rotation frequency. The SNR is improved by a factor of 5 using this approach (Figure 3).

The samples consist of 250-nm thick aluminum Archimedean spirals on high resistivity silicon that have been fabricated using electron-beam lithography (Vistec EBPG5000plus). The line width is 1 μm, the distance between turns is 4 μm, and they are arranged in a 2D rhombohedral lattice with a period of 80 μm in a 5×5 mm array, as seen Figure S1c.[25] Left-handed denotes a counterclockwise rotation when beginning at the center of the spiral and moving outward (Figure S1a), and right-handed corresponds to a clockwise rotation (Figure S1b). The samples are placed with the lithographic structures facing the incoming THz beam.

The goal of the current research is to improve the accuracy and speed of time-domain THz measurements of optical activity, ultimately extending the technique to molecular systems. In what follows, we explain a method that expands on current techniques of analyzing transmission amplitude data as a function of a few specific polarizer angles in the frequency domain. We then show that the same information may be obtained by applying this method directly to time-domain data. While these two topics are themselves of interest, they also provide the background for the final portion of this discussion: an experimental technique that dramatically improves the efficiency of these measurements.

In general, if a polarizer is placed in the beam path of vertically polarized light, the transmitted amplitude will be proportional to $\cos(\theta)$, where θ is the angle of the polarizer with respect to the x-axis (we define x to be vertical, y to be horizontal, and z to be the direction of propagation). If a second fixed polarizer is added that passes vertically polarized light as shown in Figure 1, then the signal will be proportional to $\cos^2(\theta)$, where θ is the angle of the analyzer with respect to the fixed polarizer. Finally, if a sample is present that rotates the polarization of the input pulse by an amount ϕ, the signal amplitude is given by

$$A = A^{'}\cos(\theta)\cos(\theta - \phi), \tag{1}$$

where A' is the initial amplitude. Using the identity $\cos(\theta - \phi) = \cos(\theta)\cos(\phi) + \sin(\theta)\sin(\phi)$, and letting $A_x = A^{'}\cos(\phi)$ and $A_y = A^{'}\sin(\phi)$, Eq. (1) becomes

$$A = A_x\cos^2(\theta) + A_y\cos(\theta)\sin(\theta). \tag{2}$$

In addition, it is possible to use Euler's formula, $e^{ix} = \cos x + i\sin x$, or equivalently $\cos x = 1/2(e^{ix} + e^{-ix})$, to rearrange Eq. (1) as

$$A = \frac{A^{'}}{2}\cos(2\theta - \phi) + \frac{A^{'}}{2}\cos(\phi). \tag{3}$$

These equations are valid either for the electric field at one instant in time in the time domain or for a monochromatic wave in the frequency domain. In the subsequent discussion, we explicitly specify the frequency dependence of frequency-domain quantities, e.g., $A_x(\omega)$ and $A_y(\omega)$, to distinguish them from time-domain quantities A_x and A_y. In addition, note that while we use the symbol ω to indicate frequency-dependence, we plot frequency domain spectra using linear (not angular) frequency as the abscissa. When specific frequencies are mentioned, they are also in linear terms.

If time-domain spectra are measured at a set of polarizer angles between 0° and 180°, $A'(\omega)$ and $\phi(\omega)$ can be extracted (after Fourier transforming each spectrum into the frequency domain) by using Eq. (1) as a fitting function for the data at each particular frequency value. If $A_x(\omega)$ and $A_y(\omega)$ are desired instead of $A'(\omega)$ and $\phi(\omega)$, then Eq. (2) may be used instead. Figure 2(a) is an example of using this approach to obtain $\phi(\omega)$ at a frequency of 1.23 THz, where there is a strong resonant feature from the spirals. The figure compares a blank scan (no sample present), a bare Si wafer, a wafer with left-handed spirals, and one with right-handed spirals. For each of these materials, 46 scans at polarizer angles ranging from 0° to 180° in steps of 4° were carried out. It is

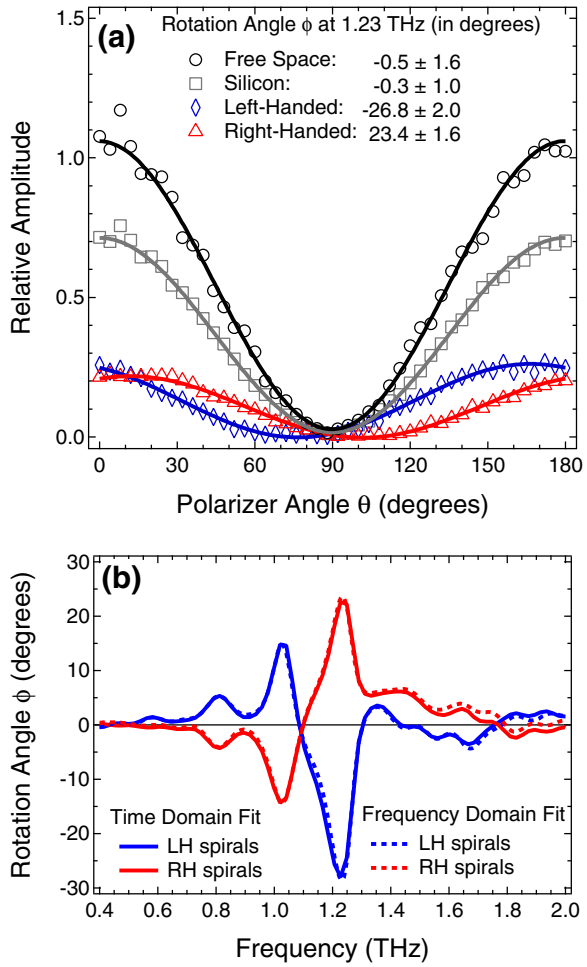

FIG. 2. The rotation angle $\phi(\omega)$ of each frequency component of a THz pulse may be determined by measuring the transmission amplitude as a function of the polarizer angle (θ). After measuring the transmission spectrum at a set of polarizer angles and transforming these spectra into the frequency domain, $\phi(\omega)$ may be obtained using the expression in Eq. (2) as a fitting function. In part (a), the value of $\phi(\omega)$ for a particular frequency (1.23 THz) is extracted from each of four sets of measurements: free space, silicon, left-handed spirals, and right-handed spirals (black circles, gray squares, blue diamonds, and red triangles, respectively). When this procedure is carried out for every frequency in the experimental bandwidth, the result is a spectrum of optical rotation angles, as shown in the dashed traces of part (b). The solid traces in part (b) of the figure illustrate the fact that the values of $\phi(\omega)$ may also be obtained by using a fitting function (Eq. (5)) in the time domain and Fourier transforming the resulting pair of time-domain amplitudes, as described in the text.

seen that $\phi(\omega)$ has equal magnitude and opposite sign for the two handednesses within the statistical uncertainty indicated. The dashed lines in Figure 2(b) correspond to the rotation angle as a function of frequency from 0.4 to 2.0 THz for left- and right-handed spirals. The rotation angle of the transmitted light has the opposite sign across the spectrum for spirals of opposite handedness. If the sample is reversed or "flipped over" such that the THz pulse traverses the silicon wafer prior to the encountering the spirals, the sign of the rotation angle is reversed as well.

It is mathematically equivalent, though perhaps less physically intuitive, to apply the same fitting procedure directly to the time-domain measurements, first determining A_x and A_y (as functions of time) and then Fourier transforming each to obtain $A_x(\omega)$ and $A_y(\omega)$. Specifically, Eq. (2) is used to fit to the measured THz amplitude as a function of θ at each time delay (instead of each frequency point) to determine A_x and A_y which are then Fourier transformed, and $\phi(\omega)$ is obtained using Eq. (5) below. This is illustrated with the solid lines in Figure 2(b), where it is seen that essentially identical results are obtained whether the fitting procedure is done in the time or frequency domain.

The advantage of using this fitting procedure instead of relying on only 2 (or 3) polarizer angles as previous workers have done is that $A'(\omega)$ and $\phi(\omega)$ or, equivalently, $A_x(\omega)$ and $A_y(\omega)$, are determined as the values of two parameters that best fit the known dependence of transmitted amplitude on polarizer angle. This avoids the necessity of certain assumptions such as that two polarizer angles are exactly 90° (or 45°) apart. Also, when using the fitting method, it is straightforward to improve the precision of a measurement by increasing the number of polarizer angles considered. The obvious disadvantage of this method is that many scans must be taken instead of two or three.

Whether the analysis is carried out in the time domain or the frequency domain, the fitting approach operates on data that consist of sets of amplitude values that vary with the polarizer angle θ. Obtaining the optimal parameters (A_x and A_y) for the function that describes this variation (Eq. (2)) requires least-squares fitting. However, by using a rapidly spinning polarizer, it becomes possible to measure A_x and A_y directly.

In this method, the rotating polarizer spins at frequency f, and $2f$ is used for the lock-in amplifier reference frequency. The angle of rotation of the polarizer, θ, is equal to ft as time, t, elapses. Through analogy with Eq. (3), it can be shown that when a polarizer is continuously rotating at frequency f, the amplitude of the signal input to the lock-in amplifier at a particular point in the time-domain THz waveform is given by

$$A_{2f} = \frac{A'}{2}\cos(2ft - \delta_{2f}) + \frac{A'}{2}\cos(\delta_{2f}), \tag{4}$$

where δ_{2f} is the phase of this wave relative to the rotating polarizer. The rotation angle of the polarization ϕ at a given time delay is equal to δ_{2f}. If a dual-channel lock-in amplifier with a reference frequency of $2f$ is used, then A_x and A_y can be read directly from the instrument at each point in the time domain. Performing a Fourier transform on A_x and A_y yields the amplitude and phase in the frequency domain for both the x and y polarizations: $A_x(\omega)$, $A_y(\omega)$, $\delta_x(\omega)$, and $\delta_y(\omega)$. Figure 3 is a plot of the time-domain x and y amplitudes of light transmitted through an array of right-handed spirals. The frequency-domain x and y amplitude spectra are shown in the inset. An estimate of the smallest measureable change in polarization state can be obtained by considering the SNR at each particular frequency. A rotation can be measured if the signal that is shifted from A_x into A_y is larger in amplitude than the noise in A_y. It is possible to obtain a SNR of ~1000:1 at the peak THz bandwidth, which corresponds to the possibility of measuring a rotation angle of 0.1°. Increasing the rotation frequency of the polarizer should further improve the SNR.

The rotation angle in the frequency domain, $\phi(\omega)$, can be obtained from these four quantities using[26]

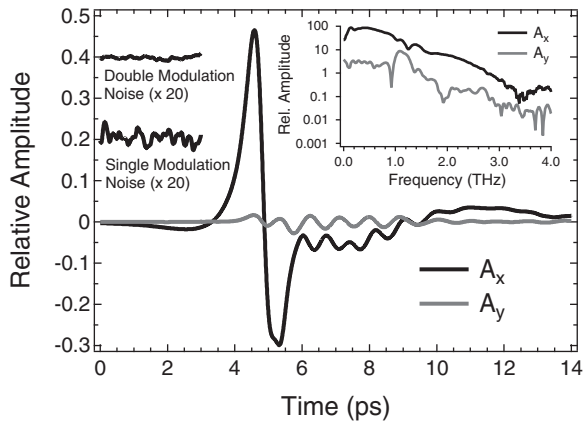

FIG. 3. A vertically polarized THz pulse has both vertical (A_x) and horizontal (A_y) amplitude components after transmission through an array of right-handed spirals. The inset displays the relative amplitudes of these components in the frequency domain. These data were collected with the continuously spinning polarizer technique described in the text. At the mid-left of the figure, the first 3 ps are shown at 20 times higher sensitivity to illustrate the improved signal to noise ratio obtained using a double-modulation variation of the data acquisition.

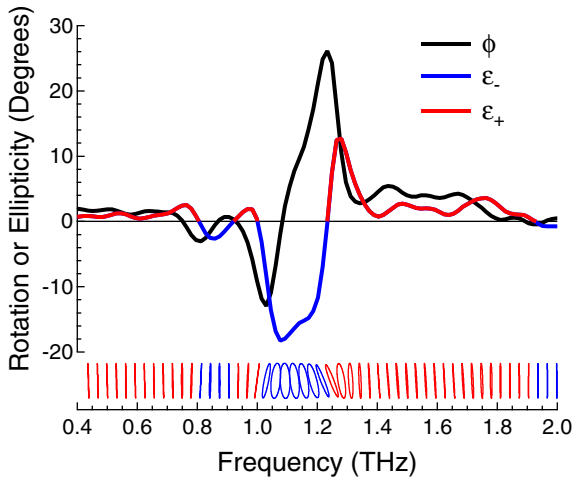

FIG. 4. The rotation angle $\phi(\omega)$ and signed ellipticity $\varepsilon_{\pm}(\omega)$ of each frequency component in the THz pulse are obtained in a single time-domain measurement using the spinning polarizer method. The values of $\phi(\omega)$ (black line) and $\varepsilon_{\pm}(\omega)$ (blue and red line) are plotted above. The same information is illustrated below the plot, where the polarization state of the light at each particular frequency is depicted. In these figures, blue indicates left-handed ellipticity and red indicates right-handed. For example, the light at 1.10 THz is left-hand elliptical but not rotated, while the light at 1.25 THz is rotated approximately 25° but is linearly polarized.

$$\tan 2\phi(\omega) = \frac{2A_x(\omega)A_y(\omega)}{A_x^2(\omega) - A_y^2(\omega)}\cos\delta(\omega), \tag{5}$$

where the phase difference is $\delta(\omega) = \delta_y(\omega) - \delta_x(\omega)$. The ellipticity angle, $\varepsilon(\omega)$, is given by $\arctan(b/a)$, where a and b are the major and minor axes of the polarization ellipse, respectively, and are obtained from[26]

$$\begin{aligned} a^2 &= A_x^2(\omega)\cos^2\phi(\omega) + A_y^2(\omega)\sin^2\phi(\omega) \\ &\quad + 2A_x(\omega)A_y(\omega)\cos\delta(\omega)\cos\phi(\omega)\sin\phi(\omega), \\ b^2 &= A_x^2(\omega)\sin^2\phi(\omega) + A_y^2(\omega)\cos^2\phi(\omega) \\ &\quad - 2A_x(\omega)A_y(\omega)\cos\delta(\omega)\cos\phi(\omega)\sin\phi(\omega). \end{aligned} \tag{6}$$

Ellipticity therefore ranges from 0° to 45°. For linearly polarized light, $\epsilon(\omega) = 0°$, and for circularly polarized light it is 45°.

Since a and b must be positive numbers, $\epsilon(\omega)$ will always be positive. However, $\delta(\omega)$ ranges from $-\pi$ to π and indicates the handedness at that frequency. It is right-handed if $\delta(\omega)$ is positive and left-handed if negative. Right-handed corresponds to the electric field vector tracing out a clockwise rotation while looking toward the radiation source, and left-handed corresponds to counter-clockwise rotation. The handedness can be conveniently included to yield the signed ellipticity, $\epsilon_{\pm}(\omega)$, by multiplying $\epsilon(\omega)$ by -1 if $\delta(\omega) < 0$ and $+1$ if $\delta(\omega) > 0$. Figure 4 plots the rotation angle and signed ellipticity for right-handed spirals. By comparing the spectrum of $\phi(\omega)$ in Figure 4 (black trace) with the equivalent spectrum in Figure 2(b) (red trace), it can be seen that the same information is obtained with both methods, despite the fact that only one time-domain measurement was required using the spinning polarizer method.

A description of the polarization state of different spectral components of the THz pulse is shown below the traces in Figure 4 (the results for left-handed spirals are shown in Figure S2a). Blue ellipses are used for frequencies at which the ellipticity is left-handed, $\epsilon_{-}(\omega)$, and red for right-handed, $\epsilon_{+}(\omega)$. Given the frequency-domain amplitude and phase, or also the polarization rotation and ellipticity, it is straightforward to compute the Stokes parameters for every spectral component in the THz bandwidth.[25] The polarization state of light at a particular frequency is sometimes represented as a point on the surface of a Poincaré sphere, but we feel that this is less intuitive than the illustration we have used here, especially for broadband measurements.

The spinning polarizer method yields the same results as traditional methods, but the data are collected much more efficiently and without requiring specialized THz emitters and detectors. This means that the technique is applicable to THz spectrometers that use electro-optic sampling rather than being limited to instruments based on photoconductive antennas. Our future work will use this method to characterize the THz optical activity of chiral molecular samples as well as a means to fully characterize the influence of spin-polarized electrons on THz emission from GaAs.[27]

We acknowledge the National Science Foundation (Grant No. CHE-0911593) for partial support of this work.

[1]P. R. Smith, D. H. Auston, and M. C. Nuss, IEEE J. Quantum Electron. **24**, 255 (1988).
[2]C. Fattinger and D. Grischkowsky, Appl. Phys. Lett. **54**, 490 (1989).
[3]M. C. Beard, G. M. Turner, and C. A. Schmuttenmaer, J. Phys. Chem. B **106**, 7146 (2002).
[4]X. Liu, S. MacNaughton, D. B. Shrekenhamer, H. Tao, S. Selvarasah, A. Totachawattana, R. D. Averitt, M. R. Dokmeci, S. Sonkusale, and W. J. Padilla, Appl. Phys. Lett. **96**, 011906 (2010).
[5]W. J. Padilla, M. T. Aronsson, C. Highstrete, M. Lee, A. J. Taylor, and R. D. Averitt, Phys. Rev. B **75**, 041102 (2007).
[6]K. J. Chau, M. C. Quong, and A. Y. Elezzabi, Opt. Express **15**, 3557 (2007).
[7]N. Kanda, K. Konishi, and M. Kuwata-Gonokami, Opt. Express **15**, 11117 (2007).
[8]A. Y. Elezzabi and S. Sederberg, Opt. Express **17**, 6600 (2009).
[9]N. Kanda, K. Konishi, and M. Kuwata-Gonokami, Opt. Lett. **34**, 3000 (2009).

[10]V. V. Kubarev, V. Y. Prinz, E. V. Naumova, and S. V. Golod, in *34th International Conference on Infrared, Millimeter, and Terahertz Waves* (IEEE Press, Piscataway, NJ, 2009), p. 867.
[11]L. D. C. Tzuang, Y. W. Jiang, Y. H. Ye, Y. T. Chang, Y. T. Wu, and S. C. Lee, Appl. Phys. Lett. **94**, 091912 (2009).
[12]G. D. Fasman, *Circular Dichroism and the Conformational Analysis of Biomolecules* (Plenum, New York, 1996).
[13]S. Abbate, E. Castiglioni, F. Gangemi, R. Gangemi, and G. Longhi, Chirality **21**, E242 (2009).
[14]P. Atkins and R. Friedman, *Molecular Quantum Mechanics*, 4th ed. (Oxford University Press, Oxford, 2005).
[15]J. Xu, J. Galan, G. Ramian, P. Savvidis, A. Scopatz, R. R. Birge, S. J. Allen, and K. Plaxco, *in Chemical and Biological Standoff Detection*, edited by J. O. Jensen and J. M. Theriault (SPIE, Bellingham, WA, 2003), Vol. 5268, p. 19.
[16]E. Castro-Camus, J. Lloyd-Hughes, M. B. Johnston, M. D. Fraser, H. H. Tan, and C. Jagadish, Appl. Phys. Lett. **86**, 254102 (2005).
[17]M. Tani, Y. Hirota, C. T. Que, S. Tanaka, R. Hattori, M. Yamaguchi, S. Nishizawa, and M. Hangyo, Int. J. Infrared Millim. Waves **27**, 531 (2006).
[18]E. Castro-Camus and M. B. Johnston, J. Opt. A, Pure Appl. Opt. **11**, 105206 (2009).
[19]T. Nagashima and M. Hangyo, Appl. Phys. Lett. **79**, 3917 (2001).
[20]R. Shimano, Y. Ino, Y. P. Svirko, and M. Kuwata-Gonokami, Appl. Phys. Lett. **81**, 199 (2002).
[21]H. Dong, Y. D. Gong, V. Paulose, and M. H. Hong, Opt. Commun. **282**, 3671 (2009).
[22]T. Hofmann, C. M. Herzinger, A. Boosalis, T. E. Tiwald, J. A. Woollam, and M. Schubert, Rev. Sci. Instrum. **81**, 023101 (2010).
[23]T. Hofmann, C. M. Herzinger, J. L. Tedesco, D. K. Gaskill, J. A. Woollam, and M. Schubert, Thin Solid Films **519**, 2593 (2011).
[24]M. R. C. Williams, A. B. True, A. F. Izmaylov, T. A. French, K. Schroeck, and C. A. Schmuttenmaer, Phys. Chem. Chem. Phys. **13**, 11719 (2011).
[25]See supplementary material at http://dx.doi.org/10.1063/1.4729148 for optical micrographs of the lithographically defined spirals, the amount of polarization rotation and ellipticity induced by left-handed spirals, and additional material pertaining to the Stokes parameters.
[26]A. Yariv and P. Yeh, *Optical Waves in Crystals* (John Wiley & Sons, New York, 1984).
[27]J. M. Schleicher, S. M. Harrel, and C. A. Schmuttenmaer, J. Appl. Phys. **105**, 113116 (2009).

Supplemental Material for:
Efficient Measurement of Broadband Terahertz Optical Activity

Daniel J. Aschaffenburg,[1)] Michael R. C. Williams,[1)] Diyar Talbayev,[1,1)] Daniel F. Santavicca,[2)] Daniel E. Prober,[2)] and Charles A. Schmuttenmaer[1,2)]

[1]Yale University, Department of Chemistry, PO Box 208107, 225 Prospect St., New Haven, CT 06520-8107 USA

[2]Yale University, Department of Applied Physics, New Haven, CT 06511 USA

May 21, 2012

This document contains optical micrographs of the lithographically defined spirals, additional material pertaining to the Stokes parameters, and the amount of polarization rotation and ellipticity induced by left- & right-handed spirals.

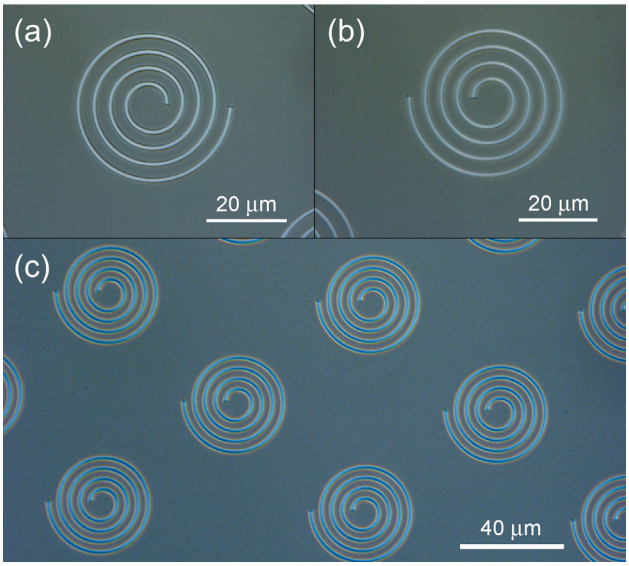

Figure S1. The samples used in these experiments consisted of periodic arrays of either left-handed or right-handed aluminum spirals on a Si substrate. Part a) displays left-handed spirals, part b) displays right-handed spirals, and part c) illustrates the rhombohedral 2-dimensional lattice.

[1] Current address: Department of Physics, Tulane University, New Orleans, LA 70118

[2]Email: charles.schmuttenmaer@yale.edu

The polarization state of light is often represented by the Stokes parameters, which are commonly expressed as combinations of linear and circular intensities as seen in the left hand column below. The Stokes parameters can also be obtained from $A_x(\omega)$, $A_y(\omega)$, $\delta_x(\omega)$, and $\delta_y(\omega)$ as shown in the middle column, and the normalized Stokes parameters can be obtained from $\varepsilon_{\pm}(\omega)$ and $\phi(\omega)$ as shown in the right hand column.[1]

$$
\begin{aligned}
S_0 &= I_x(\omega) + I_y(\omega) && = A_x(\omega)A_x^*(\omega) + A_y(\omega)A_y^*(\omega) && = 1 \\
S_1 &= I_x(\omega) - I_y(\omega) && = A_x(\omega)A_x^*(\omega) - A_y(\omega)A_y^*(\omega) && = \cos 2\varepsilon_{\pm}(\omega)\cos 2\phi(\omega) \\
S_2 &= I_{+45^o}(\omega) - I_{-45^o}(\omega) && = 2\left|A_x(\omega)\right|\left|A_y(\omega)\right|\cos\delta(\omega) && = \cos 2\varepsilon_{\pm}(\omega)\sin 2\phi(\omega) \\
S_3 &= I_{RHCP}(\omega) - I_{LHCP}(\omega) && = 2\left|A_x(\omega)\right|\left|A_y(\omega)\right|\sin\delta(\omega) && = \sin 2\varepsilon_{\pm}(\omega)
\end{aligned}
$$

S_0 is the total intensity, and S_{1-3} are differences in intensities as indicated. Figures S2a and S2b show plots of the amount of rotation and ellipticity for left-handed and right-handed spirals as presented for right-handed spirals in Figure 4 of the main text. Figures S2c and S2d display the normalized Stokes parameters for the left-handed spirals and right-handed spirals, respectively. While it is possible to plot the normalized Stokes parameters on a Poincaré sphere, which would form a trajectory in going from low frequency to high frequency, we feel that the visualization presented along the bottom of Figures S2a and S2b is easier to interpret.

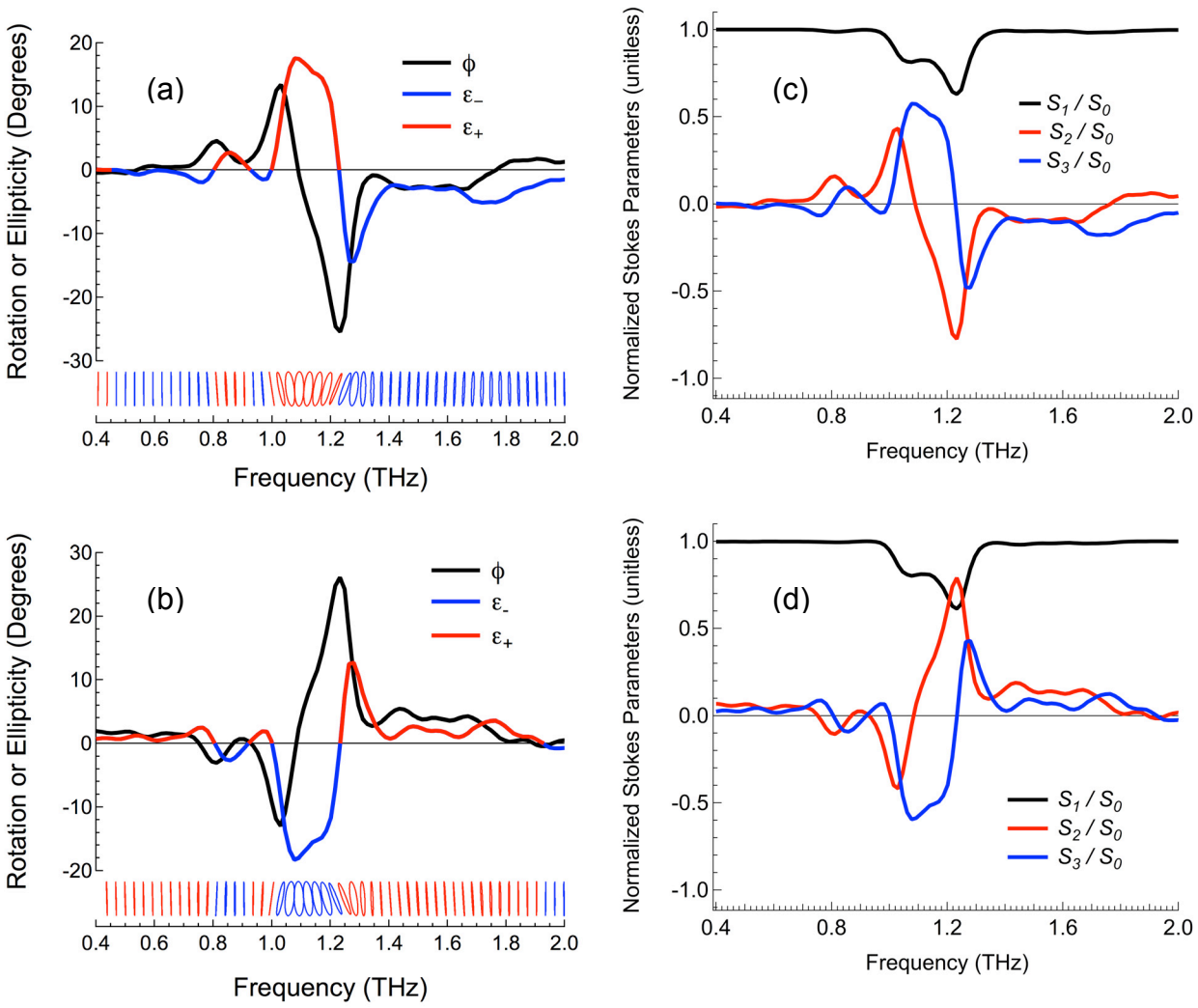

Figure S2. Parts a) and b) display the rotation angle $\phi(\omega)$ and signed ellipticity $\varepsilon_{\pm}(\omega)$ of each frequency component in the THz pulse which have been obtained in a single time domain measurement. Part a) is for left-handed spirals and part b) is for right-handed spirals. The values of $\phi(\omega)$ are shown with the black lines and $\varepsilon_{\pm}(\omega)$ are shown with the blue and red lines. The same information is illustrated at the bottom of each plot, where the polarization state of the light at each particular frequency is depicted. In these figures, blue indicates left-handed ellipticity, and red indicates right-handed. For example, the light at 1.05 THz is left-hand elliptical but not rotated, while the light at 1.25 THz is rotated approximately 25 degrees but is linearly polarized. Parts c) and d) display the normalized Stokes parameters for the left-handed and right-handed spirals, respectively. S_1 is shown in black, S_2 in red, and S_3 in blue.

References

[1]Hiroyuki Fujiwara, *Spectroscopic Ellipsometry*. (John Wiley & Sons, West Sussex, 2007).